Charge separation induces conformational changes in the photosynthetic reaction centre of purple bacteria

Günter Fritzsch,[a*] Jürgen Koepke,[a] Ralf Diem,[a] Andreas Kuglstatter[b] and Laura Baciou[c]

[a]Max-Planck-Institut für Biophysik, Heinrich-Hoffmann-Str. 7, D-60528 Frankfurt/M., Germany, [b]MRC Laboratory of Molecular Biology, Hills Road, Cambridge CB2 2HQ, UK, and [c]Centre Génétique Moleculaire, CNRS, F-91198 Gif-sur-Yvette, France. E-mail: Guenter.Fritzsch@mpibp-frankfurt.mpg.de

X-ray structures of the wild-type reaction centre from *Rhodobacter sphaeroides* have been determined to a resolution of 1.87 Å in the neutral (dark) state and to 2.06 Å in the charge-separated (light-excited) state. Whereas the overall protein structures of both states are rather similar, the domain around the secondary quinone shows significant shifts. The quinone molecule itself is observed at two different positions. In the neutral state, 55% of the quinone is located distally and 45% proximally to the cytoplasmic side. After excitation by light, however, at least 90% of the quinone is found at the proximal position. Results presented by Stowell *et al*. (1997) are confirmed, but the quality of crystallographic data has been improved. We compare the data with the structure of the mutant RC L209 PY that keeps the Q_B molecule in the proximal position even in the charge-neutral state.

Keywords: X-ray structure, secondary quinone, electron and proton transfer, membrane protein, intermediate state

1. Introduction

The reaction centre (RC) of purple bacteria (Fig. 1) is a membrane-bound pigment-protein complex that facilitates the conversion of light into electrochemical free energy. The RC core consists of two protein subunits, L and M, each containing five transmembrane helices. Four bacteriochlorophylls, two bacteriopheophytins, two ubiquinone-10 molecules (UQ_{10}), one non-heme iron (Fe^{2+}), and one carotenoid molecule are non- covalently bound by subunits L and M.

A third peptide, H, is anchored in the membrane by a single membrane-spanning helix. Except for the carotenoid and subunit H, the protein shows a quasi two-fold symmetry with its symmetry axis perpendicular to the membrane. Beginning at a periplasmically located bacteriochlorophyll dimer, the cofactors are arranged as two branches, A and B, across the membrane. One bacteriochlorophyll, bacteriopheophytin and UQ_{10} molecule, respectively, form a branch. Between the branches, the non-heme Fe^{2+} is located on the non-crystallographic symmetry axis.

After excitation by light, an electron is transferred along the A branch to the primary and finally to the secondary quinone which is converted into a semiquinone. Two protons move from the cytoplasmic side to Q_B changing it to its quinol state. The quinol dissociates from the RC complex. To analyse conformational changes generated by charge separation, X-ray data have been collected from one and the same crystal in the dark and after illumination by laser light.

2. Materials and methods

The RC from *Rhodobacter sphaeroides* was purified and crystallized as reported earlier (Baciou & Michel 1995; Ermler *et al*. 1994; Fritzsch 1998). During purification, the native ubiquinone-10 of the RC is partially lost. To ensure a fully occupied Q_B binding site, ubiquinone-2 was added to the RC in 10-fold excess, and the full occupancy of the Q_B binding site with ubiquinone-2 was confirmed spectroscopically. After dialysis against 10 mM Tris·HCl, pH 8.5, 0.1% N-lauryl-N,N-dimethyl-N-oxide (LDAO), and 180 mM NaCl, the protein was concentrated and crystallized in detergent (LDAO) micelles by applying the vapour diffusion method with sitting drops.Crystals grew in a crystallization buffer containing 1 M potassium hydrogen phosphate as precipitant, pH 8.5, 90 mM NaCl, 0.1% LDAO, 2% hexane-1,2,3-triol, 3% heptane-1,2,3-triol, 3% dioxane, and 100 µM protein in the drop as well as 2 M potassium hydrogen phosphate in the reservoir. The RCs crystallize in space group $P3_121$ with one protein molecule per asymmetric unit. Crystals appear at 21°C in about two weeks. Their maximum size is 2.0 x 1.0 x 1.0 mm^3. To achieve complete illumination and charge separation throughout the entire crystal during light exposition, a small crystal of 0.5 x 0.3 x 0.2 mm^3 has been selected for data collection.The X-ray experiments have been performed at the EMBL outstation in Hamburg at beam line BW7B. An RC crystal was equilibrated stepwise with the cryo buffer consisting of 65% crystallization buffer mentioned before and 35% glycerol. The crystal was transferred to the goniostat and cooled quickly to -150°C in a nitrogen stream. Both, resolution and mosaicity, have been improved remarkably by reversible flash-cooling (Samygina *et al*., 2000). The RC crystal was transferred four times from the cold nitrogen stream to the ambient temperature and back (10 s per cycle). A first X-ray data set has been collected at -150°C in the dark. Afterwards the crystal was thawed for 10 s and exposed for 5 s to light of 594 nm wavelength from a helium-neon-laser.

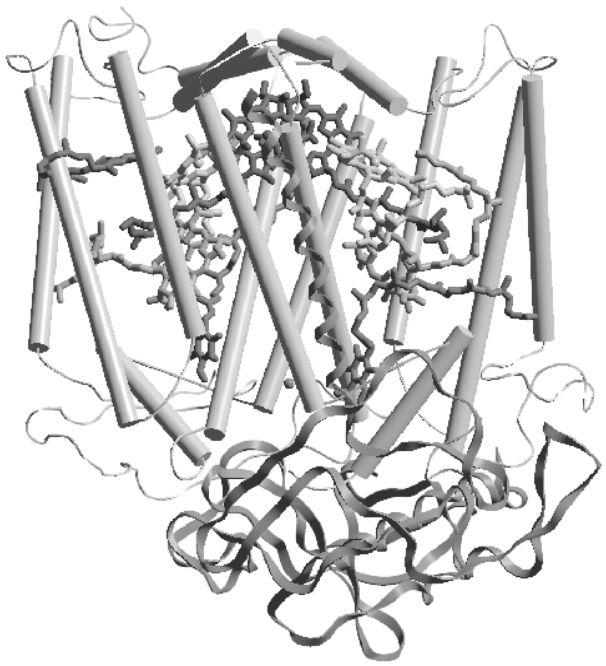

Figure 1

The wild-type reaction centre of the purple bacterium *Rhodobacter sphaeroides*. The periplasmic side is above, the cytoplasmic below. The protein helices of the L and M subunits are indicated by cylinders. The H-subunit (below) is represented as ribbons as well as its membrane-spanning helix. The cofactors are shown as stick models. The bacteriochlorophyll dimer is located close to the top and the two branches A and B of cofactors are spread right and left inside this view of the RC molecule. The head-group of the secondary quinone can be seen at the lower end of the left (B) branch.

The light-excited state of the RC was "frozen" and another data set has been collected with this crystal. During the collection of the "light" data set, the laser was switched off. Simultaneous exposure with laser light and X-rays destroys the crystal after a few images. The illuminated crystal belongs to the same space group as before, but it has a slightly larger unit cell of the size a = b = 140.0 Å, c = 184.8 Å, compared to a = b = 138.7 Å, c = 184.6 Å obtained in the dark.

Data sets were processed with DENZO and merged using SCALEPACK, both from the HKL program suite (Otwinowski & Minor, 1997). Structure factors were calculated from the measured densities employing TRUNCATE of the CCP4 (Collaborative Computational Project Number 4, 1994). Starting with the model deposited in the Protein Data Bank with accession code 1PCR (Ermler *et al*., 1994), the refinement was performed using Refmac5 (Murshdov *et al*., 1999). The geometry was restrained to the standard Engh & Huber (1991) values. Data were used to a resolution of 1.87 Å for the dark and to 2.07 Å for the light data set. Firmly bound water molecules were added by detecting peaks >3σ in the F_o-F_c difference density map with geometry suitable for hydrogen bonding. Between each refinement round, $2F_o$-F_c and F_o-F_c electron density maps were inspected using the graphics program XtalView (McRee, 1999). The crystallographic data are listed in Table 1.

Table 1 Data collection and refinement statistics

	Dark state (neutral)	*Light-excited state (charge separation)*
Data collection		
Resolution (Å)	1.87	2.07
Unique observations	147217	123115
Average I/σ(I) (last shell)	23.7 (2.8)	10.8 (2.2)
R_{sym} (last shell) (%)	3.9 (20.1)	9.8 (32.8)
Completeness (%)	87	96
Redundancy	1.9	2.5
Refinement		
R_{cryst} (%)	17.7	20.4
R_{free} (%)	19.5	22.4
Mosaicity	0.39	0.39

3. Results

In the work of Stowell *et al.* (1997), the neutral data set was refined to 2.2 Å and the charge separated data set to 2.6 Å (R_{free} values 27.0% and 29.9%, respectively). In contrast, the data presented here yield 1.87 Å and 2.07 Å resolution and R_{free} values of 19.5% and 22.4%, respectively. In both structures, the position of the primary quinone, Q_A, is practically identical. Figure 2 shows the well-shaped electron density for this cofactor. The quinone oxygen of Q_A, located proximally to Fe^{2+}, is hydrogen bonded to the side chain of His M219 (on the left in Fig.2) while the distal oxygen forms a hydrogen bond to the backbone nitrogen of Ala M260 (on the right in Fig. 2). Different distances of both hydrogen bonds have been refined in earlier models. Since asymmetric binding of the primary semiquinone was postulated by FTIR (Brudler *et al*., 1994; Breton *et al*., 1994) and EPR analyses (van den Brink *et al*., 1994), the precise position of Q_A became a subject of interest. In the present structure the Q_A head-group is located symmetrically between the hydrogen bonded residues, both distances amounting to 2.75 Å (with r.m.s. of 0.2 Å) in the neutral as well as in the charge-separated state. In both states, Q_A itself is not charged.

In contrast to Q_A, the Q_B molecule is found at two different positions, located distal or proximal to the cytoplasmic side (Figs. 3 and 4). In the neutral state, the distal position is occupied by 55% and the proximal position by 45%, however in the charge-separated state the occupancies are 10% and 90%, respectively. The distance between the two positions is ~ 4.5 Å. The translation of Q_B between both positions is accompanied by a rotation of the Q_B head-group by 180°. The hydrogen bonding of the neutral state corresponds to the pattern that was found earlier for trigonal RC crystals (Ermler *et al*., 1994). The hydrogen bond between the backbone nitrogen of Ile L224 and Q_B, observed in all dark structures of the *Rhodobacter sphaeroides* RC, is confirmed again. In the charge-separated state, this bond length increases from 2.4 Å to 3.4 Å, and a strong hydrogen interaction appears between His L190 and the proximal keto-oxygen of Q_B as indicated by the bond length of 2.55 Å. In the light structure of Stowell *et al.* (1997) this distance is 2.8 Å. A strong interaction between Q_B and His L190 facilitates the electron transfer from Q_A^- to Q_B as His L190 is coupled to Fe^{2+} (2.1 Å) .

The hydrogen bond between Asp L213 and Ser L223, observed in the dark structures of Ermler *et al.* (1994) and Stowell *et al.* (1997), is confirmed. This bond is maintained also after charge separation. Another hydrogen bond, formed between Gly L225 and Q_B, exists only in the charge-separated state. A rather weak hydrogen bond is observed in the light structure between Thr L226 and Q_B, which are separated by 3.5 Å (3.2 Å in the corresponding structure of Stowell *et al.* (1997)). The electron density of the Q_B molecule in the proximal position is not sharp enough to decide whether the quinone is rotated by 180° relatively to the distal position as claimed in the study of Stowell *et al.* (1997). The arrangement of the amino acids in the charge-separated state, however, does not allow another orientation.

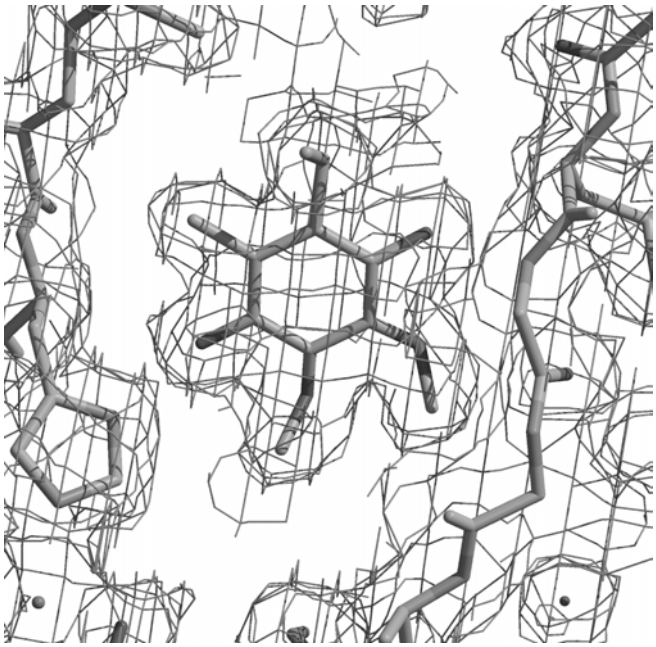

Figure 2

Electron density map (1 σ) of the Q_A head-group and its surrounding residues. The quinone model fits well into the electron density.

4. Discussion

The objective of this study is the analysis of conformational changes in the RC near the secondary quinone upon excitation by laser light (charge separation). In the neutral (dark) state of the wild-type RC,

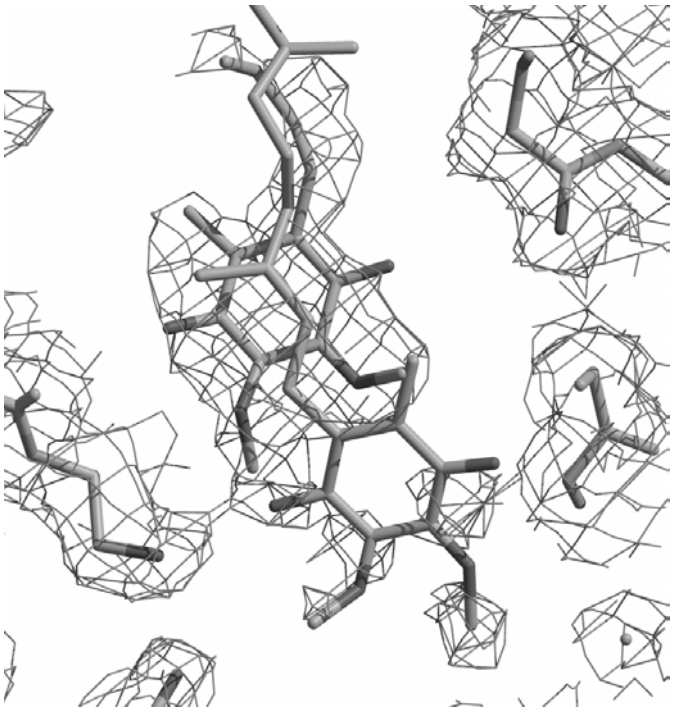

Figure 3

Electron density map (1 σ) of the Q_B head-group in the neutral (dark) state. The two refined models of the Q_B head-group for the distal (above) and the proximal (below) positions are shown. In this state the distal position is higher (55%) occupied than the proximal one (45%). The two head-groups are almost in plane, however, they are twisted about the isoprene chain by 180°.

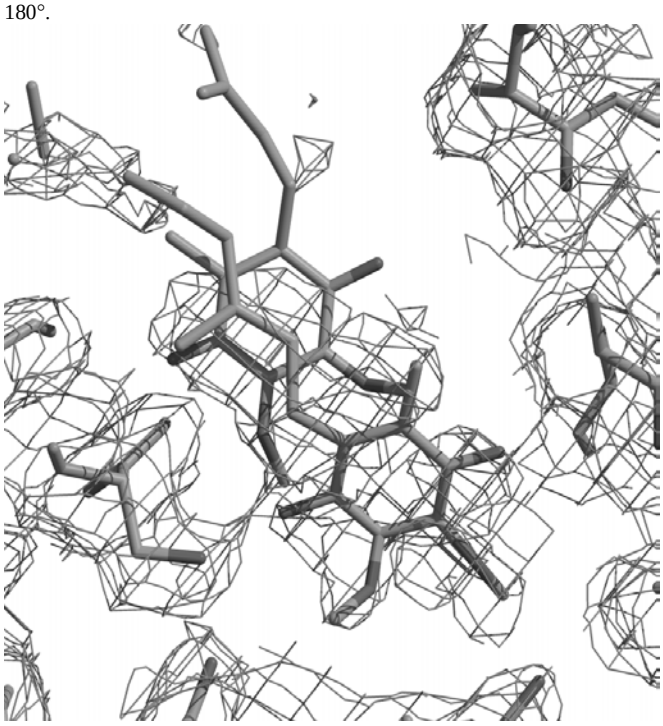

Figure 4

Electron density map (1 σ) of the Q_B head-group in the charge-separated state. The models of the Q_B head-group for the distal (above) and the proximal (below) positions are shown. In this state the distal position is lower (10%) occupied than the proximal one (90%). The two head-groups are twisted about the isoprene chain by 180°.

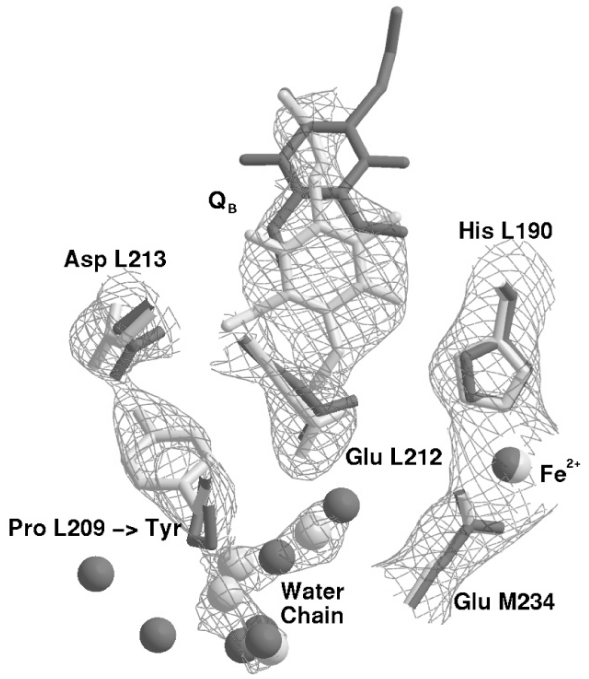

Figure 5

Electron density map near the Q_B binding site of the mutant RC L209PY. Two models of the quinone molecule are represented. The upper (dark) quinone head-group indicates the position of the Q_B head-group in the neutral state of the wild-type RC whereas the lower (light) quinone head-group shows the position of the Q_B head-group in the neutral state of the mutant RC L209PY.

the Q_B is predominantly bound at a position distal to the cytoplasmicside (Ermler *et al.* 1994, Stowell et al. 1997). Upon excitation by light an electron is transferred from a bacteriochlorophyll dimer to the secondary quinone forming a negatively charged Q_B^- molecule. The spatial order of the electrostatic potential in the vicinity of the Q_B binding pocket is changed and the secondary quinone, in its negatively charged form, favours the proximal binding position. Furthermore, the arrangement of the amino acid residues near Q_B in the charge-separated state suggests a ring flip of the plane of the Q_B head group about the isoprene chain. The hydrogen bond pattern is similar to the one observed in the work of Stowell *et al.* (1997). The changed pattern of interactions between the secondary quinone and its surrounding amino acid residues in the charge-separated state indicates that the influence of the redox properties of Q_B on its environment is rather complex.

A remarkable mutant RC has been refined recently, in which Q_B is located proximally even when the X-ray data have been collected in the dark (neutral) state (Fig. 5, Kuglstatter *et al.*, 2001). In that work, the amino acid Pro L209, which is situated about 9 Å from Q_B, has been replaced by tyrosine, phenylalanine, and glutamic acid, respectively. The Q_B molecule in the neutral state has been found in three different positions. Remarkably, in the tyrosine mutant, the Q_B head-group is observed in the proximal position. This finding indicates that the position of the secondary quinone does not solely depend on the oxidation state of Q_B. A thorough analysis of the conformational changes, which Q_B undergoes during the photocycle, requires the study of the effects of pH, redox potentials, hydrophobicity and others on the position and orientation of the secondary quinone.

Acknowledgments

We thank Ilme Schlichting (Max-Planck-Institut für molekulare Physiologie, Dortmund, Germany) and Kelvin Chu (University of Vermont, Burlington, VT, USA) for their support in developing suitable conditions for data collection at cryogenic temperatures. We acknowledge help by the staff of EMBL Outstation in Hamburg, Germany, and the "European Community - Access to Research Infrastructure Action of the Improving Human Potential Programme to the EMBL Hamburg Outstation, contract number HPRI-CT-1999-00017". We thank finally for the support by PROCOPE Grant D/9822825.

References

Baciou, L. & Michel, H. (1995). *Biochemistry*, **34**, 7967-7972.
Breton, J., Boullais, C., Burie, J. R., Nabredyk, E. & Mioskowski, C. (1994). *Biochemistry*, **33**, 14378-14386.
Brudler, R., de Groot, H. J. M., van Liemt, W. B. S., Steggerda, W. F., Esmeijer, R., Gast, P., Hoff, A. J., Lugtenburg, J. & Gerwert, K. (1994). *EMBO J*. **13**, 5523-5530.
Collaborative Computational Project, Number 4 (1994). *Acta Cryst*. D**50**, 760-763.
Engh, R. A. & Huber, R. (1991). *Acta Cryst*. A**47**, 392-400.
Ermler, U., Fritzsch, G., Buchanan, S. K. & Michel, H. (1994) *Structure*, **2**, 925-936.
Fritzsch, G. (1998). *Methods Enzymol*. **297**, 57-77.
Kuglstatter, A., Ermler, U., Michel, H., Baciou, L. & Fritzsch, G. (2001). *Biochemistry*, **40**, 4253-4260.
McRee, D. E. (1999). *Practical Protein Crystallography*. San Diego, London, Boston, New York, Sydney, Tokyo, Toronto: Academic Press.
Murshudov, G. N., Lebedev, A., Vagin, A. A., Wilson, K. S. & Dodson, E. J. (1999). *Acta Cryst*. D**55**, 247-255.
Otwinowski, Z. & Minor, W. (1997). *Methods Enzymol*. **276**, 307-326.
Samygina, V. R., Antonyuk, S. V., Lamzin, V. S. & Popov, A. N. (2000). *Acta Cryst*. D**56**, 595-603.
Stowell, M. H. B., McPhillips, T. M., Rees, D. C., Soltis, S. M., Abresch, E. & Feher, G. (1997). *Science*, **276**, 812-816.
van den Brink, J. S., Spoyalov, A. P., Gast, P., van Liemt, W. B. S., Raap, J., Lugtenburg, J. & Hoff, A. J. (1994). *FEBS Lett*. **353**, 273-276.